Dual Array Microstrip Patch Antenna for Next Generation 5G Applications: A Numerical Approach

Anik Paul[a], Shubhanwita Dey Swasty[a], Tanzeem Mostafiz[a], Aysha Siddika Prity[a], Saiful Islam[a], Tanveer Ahsan[b], Md. Zulfiker Mahmud[c*]

[a]*Department of Information and Communication Technology, Faculty of Science and Technology, Bangladesh University of Professionals, Dhaka, Bangladesh*
[b]*Department of Computer Science and Engineering, International Islamic University Chittagong (IIUC), Chittagong, Bangladesh*
[c]*Department of Computer Science and Engineering, Faculty of Science, Jagannath University, Dhaka, Bangladesh*
**Corresponding author: zulfiker@cse.jnu.ac.bd*

Received: 6 February 2025; Accepted: 2 April 2025; Published: 31 July 2025

ABSTRACT

The advent of 5G technology requires significant advances in the design of antennas, particularly in the Microstrip patch antennas, which are crucial to meet the strict demands of modern telecommunications. Recent developments have emphasized the improvements in bandwidth, gain, and efficiency, particularly through the integration of dual antenna matrices into a single substrate. The proposed array antenna effectively addresses these limitations, improving performance through improved radiation characteristics and a broader bandwidth, thus facilitating the deployment of more efficient and reliable 5G communication systems. This antenna consists of two 1×9 arrays positioned at the opposing edges of the substrate, optimized for operation in the broadside direction, which operates in the range of 26 – 29 GHz with achieving a wide bandwidth of 3 GHz. CST microwave studio software is utilized to design, simulate, and optimize the antenna structure. Initially, a single-element antenna design is designed, and sequentially, 1×4 array and 1×9 array structures are designed. Finally, the present design of a 2×9 array is developed and optimized to achieve an operating frequency of 28.73 GHz with gain and efficiency of 5.54 dB and 82.7%, respectively. Therefore, the proposed microstrip patch antenna not only meets the immediate bandwidth and obtains 5G application requirements but also search the way for future innovations in wireless communication technologies.

Keywords: Dual array design; wideband; millimeter wave antenna; Microstrip patch antenna

1. INTRODUCTION

To meet the requirements of faster data rates, reduced latency, and increased network capacity, antenna architectures have evolved due to the advancement in fifth-generation (5G) wireless communication technology. Among them, the 28 GHz band dual-array antenna is one of the most attractive candidates for future 5G antennas because it can operate at a millimeter-wave frequency band that can achieve a high data rate. To develop and optimize new antennas, simulation modeling must be carried out since it allows engineers to investigate performance parameters like radiation pattern, gain and efficiency factors. Design practice, key features, and potential applications of a 28 GHz dual-array antenna in rapidly evolving field of 5G technology are investigated using this paper's simulation modelling study. Using sophisticated modeling tools, we hope to improve the efficiency and dependability of these antennas, opening new avenues for wireless communication and facilitating a smooth transition into upcoming 5G networks. Girjashankar et al. (2022) proposed a rectangular dielectric resonator-based, quad-elements MIMO antenna using substrate integrated waveguide (SIW) for millimeter-wave 5G, achieving dual-band operation (24.50–27.50 GHz and 33–37 GHz), high isolation without extra techniques, peak gain of 9.9 dB, and excellent MIMO diversity performance, validated by prototype measurements. This research introduces a dual-band MIMO antenna for 5G millimeter-wave applications, featuring two mono-poles at 27 GHz and 39 GHz, optimized for minimal mutual coupling, showing gains of 5 dBi and 5.7 dBi and efficiencies of 99.5% and 98.6%, respectively, with a very low envelop correlation and a diversity gain of about 10 dB, validated through both simulation and measurements (Ali et al., 2020). This work introduces a dual-band mmWave MIMO antenna system for 5G, featuring four E-shaped patch elements on a Rogers-5880 substrate achieving 28 dB isolation,

with resonances at 28 GHz and 38 GHz, meaning gains of 7.1 dBi and 7.9 dBi, and high performance validated by both simulation and measurement (Raheel et al., 2021). This paper details the design of a square-slotted microstrip patch antenna at 37 GHz for mmWave 5G communication, achieving a −43.05 dB return loss, 8.18 dB gain, and 16.22% impedance bandwidth using CST Microwave Studio on a Rogers RT5880 substrate (Shamim et al., 2021). This article presents two high-gain, no side lobe, 5G antenna arrays on a single substrate, achieving up to 17.3 dB gain and operating between 31.3 GHz and 39 GHz for enhanced mobile and broadcast communication (Tahseen et al., 2021). This paper details the design of a compact mmWave antenna for 5G applications, measuring 10×10×0.245 mm^3, resonating between 33 GHz and 43 GHz, with a return loss of -22 dB, simulated using CST software to meet 5G performance criteria (Oras Ahmed Shareef et al., 2022). Sehrai et al. (2020) described a compact quad-element MIMO antenna with a wide 23-40 GHz bandwidth for 5G, featuring high gains and efficiencies, strong isolation, and excellent MEG and ECC metrics, validated through prototype testing and CST simulations. In this article, K. (2021) presented a highly compact crown slot patch antenna for 28GHz and 34GHz applications, featuring a heptagon radiator with a crown-shaped slot, achieving broad bandwidths and efficient performance tailored for 5G and satellite communications. This paper introduces a high-gain, high-efficiency, low-profile rectangular patch antenna with a rectangular slot for 30 GHz 5G communication, designed on a compact Rogers Substrate, achieving a gain of 10 dBi and over 98% efficiency without complex modifications, making it ideal for 5G wireless systems (Ahmad et al., 2020). This article introduces a compact antenna for 5G mm-wave applications using a new microwave dielectric ceramic substrate, achieving an impedance bandwidth of 2.66 GHz, an average gain of 5.44 dB, and 93% radiation efficiency, optimized for the 28 GHz band (Rahman et al., 2016). This paper reviews three emerging multiple antenna technologies—cell-free massive MIMO, beam space massive MIMO, and intelligent reflecting surfaces—that could significantly enhance data rates and reliability beyond 5G networks, providing a foundation for future research (Zhang et al., 2020). This paper presents a compact, wideband flexible monopole antenna designed on a Kapton polyimide substrate for wearable applications, featuring a 1.707 GHz bandwidth, optimized performance using genetic algorithms and particle swarm optimization, and validated through measurements including on-body testing and specific absorption rate assessment for safety (Qas Elias et al., 2020). This paper discusses the design of a wideband strip helical antenna for 5G and other wireless applications, featuring a 2.41 GHz bandwidth, 11.2 dB gain, and circular polarization, designed on a Teflon substrate and optimized using CST software for applications in wideband and ultra-wideband communications (Zeain et al., 2020). This paper investigates a microstrip patch antenna operating at 28 GHz on a Rogers RT/Duroid5880 substrate, offering superior performance metrics such as a -38.348 dB return-loss and 8.198 dB gain, positioning it as an effective candidate for future 5G communications (Rana & Rahman, 2022). This paper presents a compact circularly polarized patch antenna with a meandering probe and truncated patches, achieving a 42.3% impedance bandwidth and 16.8% axial ratio bandwidth, suitable for 5G Wi-Fi and satellite communications (Lin et al., 2014). This paper presents a novel 28 GHz antenna solution for 5G cellular communications, validated through extensive measurements and simulations for effective performance in realistic environments (Hong et al., 2014). This article explores the development of large-scale antenna arrays for mmWave 5G cellular devices, detailing the design and implementation of a novel 28 GHz phased array antenna with extensive coverage, culminating in a unique cellular phone prototype with 32 antenna elements tested for effective mmWave communication and biological safety compared to 3/4G devices (Hong et al., 2014). This paper introduces a miniaturized, circularly polarized patch antenna with enhanced beamwidth for 5G mobile phones, achieving significant size reduction and comprehensive coverage by incorporating loading slots, a surrounding dielectric substrate, and a supportive metallic block (Mak et al., 2014). This paper introduces a new tapered H-shaped ground technique to significantly reduce the height of a magneto-electric dipole antenna for 5G Wi-Fi applications, using cost-effective multi-layer PCB technology, achieving an 18.74% impedance bandwidth with stable radiation patterns (Lai & Wong, 2015). This paper presents a hybrid antenna designed for 4G/5G MIMO applications, featuring separate modules for 4G and 5G frequencies, demonstrating near-ideal channel capacity and detailed performance metrics through experimental results (Ban et al., 2016). Tahseen, Zheng, and Yang (2021) proposed a modified circular patch antenna inspired by the Rotman lens structure, using square-shaped metallic rings for gain enhancement, designed for 28 GHz frequency applications in satellite and 5G

communication, with comprehensive simulation results using HFSS software. In this article, Lai and Wong (2015) presented a novel ultra-wideband (UWB) antenna based on an inverted F patch with coupled feeding, designed for 5G smartphones, achieving a 60.8% impedance bandwidth (3.27-6.13GHz) that covers specific 5G and WiFi bands, with radiation efficiency ranging from 76.0% to 91.7% across its operational spectrum. This paper describes a compact elliptical dual-band microstrip antenna with a coplanar waveguide feed, designed for 28GHz and 38GHz 5G bands using bi-layer Roger's substrates, enhanced with F-shaped slots in the ground plane to improve performance, achieving a bandwidth of 4.14GHz and a constant 6dB gain, analyzed using HFSS software (Mpele, Mbango, & Bernard, 2019). This paper presents a triple rectangular slotted microstrip patch antenna designed for WLAN at 2.4GHz and WiMAX at 3.6GHz using CST Software, featuring slots that provide appreciable gain and directivity and utilizes FR-4 substrate with a permittivity of 4.3 (Ray & Shrivastava, 2018). This paper explores the design of a microstrip patch antenna for 5G applications, enhancing performance through slots in the radiating patch to increase gain, radiation pattern, and bandwidth in the 5-6GHz range, using FR4 substrate for a compact and cost-effective solution (Tarpara, Rathwa, & Kotak, 2018). This paper presents the design and analysis of a square-shaped microstrip patch antenna array for 5G communication, operating at 10.21GHz and designed on Rogers RT Duroid 5880 substrate using CST software, achieving a fractional bandwidth of 1.62% and reflection coefficient of -14.341dB, with detailed performance analysis including the impact of substrate thickness on antenna operation (Toma, Shohagh, & Hasan, 2019). This paper introduces a dual-band antenna for 5G applications, combining a meta surface at the S-band and a partially reflective surface at the Ka-band through characteristic mode analysis. It features microstrip-fed and substrate-integrated waveguide-fed slots, forming a Fabry-Perot resonator antenna that shows bandwidths of 23.45% and 9.76% with gains ranging from 7.27 to 10.44 dBi at S-band and 11.8 to 14.6 dBi at Ka-band (Li & Chen, 2020). With an emphasis on time-domain considerations for UWB system design, this study gives an overview of UWB antenna designs while highlighting key wireless system features such as transient gain, group delay, dispersion, and polarization diversity (Adamiuk, Zwick & Wiesbeck, 2012). Experimental and simulated findings closely coincide with a gain-enhanced antipodal Vivaldi antenna for 5G communication that incorporates meta-material and corrugations. It achieves a gain of 9.53 dB and covers 5G frequency ranges from 25 to 29.5 GHz and 31.8 to 33.4 GHz (Dixit & Kumar, 2019). Using SIW technology, dual-element arrays, and extension structures, the paper suggests a directional horn antenna for compensating mmWave broadcast signal attenuation. This antenna achieves a maximum gain of 8.06 dB and nearly 2 GHz bandwidth with a gain greater than 6.5 dB, providing a reference for improving directional antennas in 5G millimeter wave bands (Hong et al., 2021)

Table 1. Comparison of present study with related works

Reference	Frequency Range	S-parameter	Max Gain	Efficiency Total
(Oras Ahmed Shareef et al., 2022)	33 - 43 GHz	-28 dB (approx.)	8.3 dB	85%
(Sehrai et al., 2020)	23 - 40 GHz	-44.5 dB	12 dB	70%
(Ahmad et al., 2020).	29.5 - 30.5 GHz	≤-10 dB	10 dB	98%
(Tahseen, Zheng, & Yang, 2021)	31.3 – 39 GHz	-26 dB	12.91 dB	-
Our work	**26 - 29 GHz**	**-26.21 dB**	**5.54dB**	**83%**

2. METHODOLOGY

2.1 Description of design

The main structure of the antenna consists of interconnected traces on the PCB, forming a specific geometric pattern. It is completely made of PEC material. The ground of the antenna is also made of PEC material. The traces, which are conductive pathways on the PCB, are arranged with gaps between them. These gaps are likely intentional and contribute to the antenna's performance characteristics. The design includes slots and holes within the traces. These features are strategically placed and sized to influence the antenna's electrical properties, such as resonance frequency or impedance matching. There are feed lines visible at the edges of the antenna structure. These lines serve to connect the antenna to the electronic circuitry, facilitating the transmission or reception of electromagnetic signals. The antenna is fabricated on a substrate material, which is typically a dielectric material (ROGERS RT-5880).

To determine if it can provide the necessary output at the necessary frequency, a single antenna element was first developed. Two single thin rectangular slots were cut on the right and left sides of the patch, and a circle was cut at the center of the single element. Despite providing a respectable s1.1 value, this design did not reach the desired frequency. After that, a 1×4 array was created to see the results. The only changes made were to the number of patches and the breadth of the substrate and ground; the materials and design remained the same. The center patch was removed from the 1×4 antenna array, leaving two identically designed patches on the left and right sides. Although it didn't happen in the intended frequency range, the outcome with this configuration was slightly better. Consequently, a single 9-array antenna was created, and this time, the intended frequency range was reached. However, in this case, the array's architecture was somewhat altered. Two distinct single antenna elements are now present in the array antenna. The new element has two additional thick rectangular slots on the left and right sides, and it is based on the primary single antenna element. The previous design is still in use at patch locations 1, 3, 7, and 9, while the new design is used at 2, 4, 5, 6, and 8 patch places. This design greatly enhanced the outcome and gave us the desired results. With this in mind, we created the 2×9 double array antenna using the same design, and we were able to obtain exceptional s-parameter values. In the 2×9 antenna arrays, the only change is that the 1×9 antenna array is mirrored in the substrate by increasing the substrate length, and the ground is also changed. The ground is 0.25mm under both ports, and it is basically also mirrored.

2.2 Structure's parameters and images

Table 2. List of parameters used in CST Microwave studio

Description	parameters	2×9 Array (mm)	1×9 Array (mm)	1×4 Array (mm)	Single Antenna Element (mm)
Patch length	pl	2.34	2.34	2.34	2.34
Patch width	pw	3.12	3.12	3.12	3.12
Substrate length	sl	9	6	6	5.43
Substrate width	sw	30.5	30.5	16.84	4.21
Substrate height	hs	0.254	0.254	0.5	0.5
Ground width	gw	30.5	30.5	16.84	4.21
Ground length	gl	0.25	6	6	5.43
Ground height	gh	0.035	0.035	0.035	0.035
Feed line length	fl	1.413	1.413	1.413	1.413
Feed line width	fw	0.543	0.543	0.543	0.543
Inset gap	ig	0.1003	0.1003	0.1003	0.1003
Circle slot radius	csr	0.40	0.40	0.40	0.40
Series line width	slw	0.543	0.543	0.543	-
Thin rectangular slot width	trsw	0.10	0.10	0.10	0.10

Thin rectangular slot length	trsl	2.0	2.0	2.0	2.0
Thick rectangular slot width	tkrsw	0.60	0.60	-	-
Thick rectangular slot length	tkrsl	2.0	2.0	-	-

This table contains all of the main structure's parameters as well as the supporting structure that were developed in order to achieve the intended results.

Figure 1. (a) single antenna element, (b) 1×4 Array, (c) 1×9 Array, (d) 2×9 Array front view, and (e) 2×9 Array back view.

Fig 1 shows how to obtain the current antenna structure. (a) shows the initial design of this work, which is a single antenna element. To improve the result, a 1x4 version was designed (b). After more changes were made to the design, the following one was produced (c). This design featured a new design for a single antenna element. In order to achieve better results at the intended frequency, the antenna's current structure (d) and (e) were developed. In 2.1 the development process is discussed in detail.

2.3 Structure optimization

Executing the processes below, we optimized the structure to the current state. This state provides the best outputs the antenna can give.

2.3.1 Effects of substrate height (hs). Here different substrate heights are taken to see which gives the best result in the desired frequency range and at the resonant frequency (28.73 GHz). It is known that the lower the substrate height, the harder it is to match the impedance, which easily leads to a bad reflection coefficient result. Besides, thin substrates have bad thermal management, leading to lower-quality performance. On the other hand, thick substrates have significant dielectric loss if not designed properly; besides, there's a possibility of distortion due to increased surface waves.

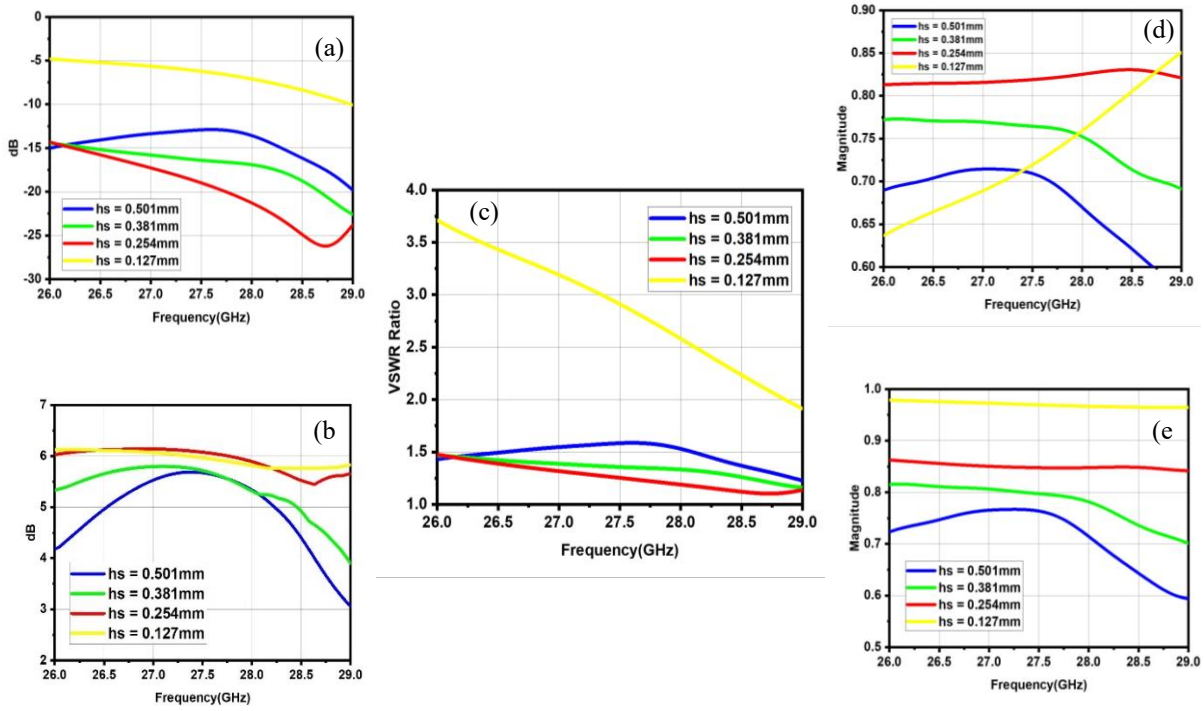

Figure 2. Comparison of (a) s-parameter, (b) gain, (c) vswr, (d) total efficiency and (e) radiating efficiency after varying substrate height (hs).

Fig 2 shows the comparison of different results after changing hs of the antenna array. Four different substrate heights (hs) are taken for comparison. These substrate heights are industry-available heights of the RT/droid 5880. The s-parameter comparison is shown in the first plot (a). There, across the entire bandwidth, the s-parameter value is good for hs=0.254 mm, but for other hs, it is bad. For hs=0.127 mm s-parameter is worse and unusable. Gain curve (b) is also consistent across the entire bandwidth for the used hs, while for others, it is not. Here, hs=0.127 mm is showing quite a good result, but it's of no use as its s-parameter value is outside the working range. In all other comparisons, hs=0.127 mm is also insignificant. VSWR comparison (c) shows the taken hs is best when compared to other values. Total efficiency comparison (d) also shows that taken hs is the best among other hs taken, and total efficiency is always above 80%. Radiating efficiency (e) is also best for the height taken. From all the comparisons it is seen that the taken height (0.254 mm) increases the antenna's performance greatly while others fail to do that.

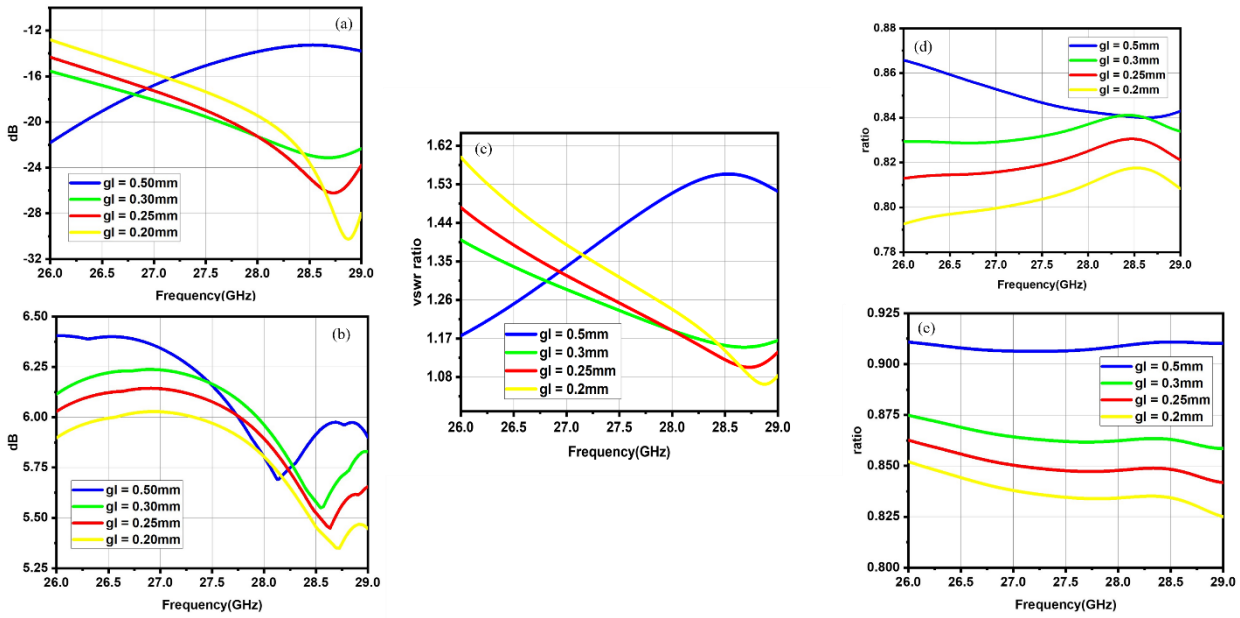

Figure 3. Comparison of (a) s-parameter, (b) gain, (c) vswr, (d) total efficiency and (e) radiating efficiency after varying ground length.

2.3.2 Effects of ground length(gl). Figure 3 shows the impact of the ground length (gl) variation on the performance characteristics of the proposed antenna. Variation in the value of gl considerably affects the resulting performances. Plot (a) shows the S-parameter curve that is stable across the entire band with a variation of the given gl of 0.25 mm. In the same way, the curve exhibits stability for gl 0.20 mm, and 0.30 mm, with the suboptimal performance at the gl = 0.50 mm. At resonance frequency, gl = 0.20 mm yields better results than the recommended value of gl. However, considering the total bandwidth the recommended gl of 0.25 mm outperforms the rest of the values of gl. In the gain comparison (b), the observed results are similar for all gl values, but at the resonant frequency, gl = 0.50 mm and 0.30 mm perform better compared to the proposed value. From the VSWR ratio comparison (c), gl = 0.20 mm shows better performance than the proposed gl. As for total efficiency (d) and radiating efficiency (e), the best performance is at a ground length (gl) of 0.50 mm, while other values of gl show almost the same results. From the above five comparative results, after a detailed study, it can be concluded that the optimal value of ground length for the proposed antenna is the available value of 0.25 mm because this configuration presents the most balanced performance for all studied parameters. This shows that small variations in the ground length can severely affect the total efficiency and effectiveness of the antenna. So, the optimization of gl is a necessity for microstrip patch antennas, especially when it comes to specific application requirements. The comparison highlights the importance of a careful adjustment of antenna parameters in order to meet the desired performance over a large frequency band.

3. RESULTS

The reflection coefficient, transmission coefficient, and frequency are presented in Fig 4. The graph shows the ability of the antenna to transmit power at various frequencies. From the graph, it is observed that the reflection coefficient is good across the entire bandwidth. At a resonant frequency of 28.73 GHz, the reflection coefficient value is -26.21 dB. In the entire band, it is lowest, between 28.5 to 29 GHz, where the value is less than -26 dB. So, the antenna reflects the signals quite well. The transmission coefficient is also stable across the entire band, and at 28.73 GHz, it is -17.34 dB. The bandwidth is above 3 GHz and covers the 26 to 29 GHz range easily.

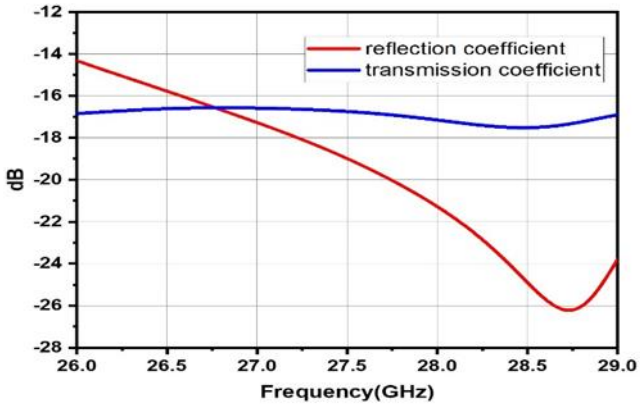

Figure 4. s-parameter of proposed 2 × 9 array antenna.

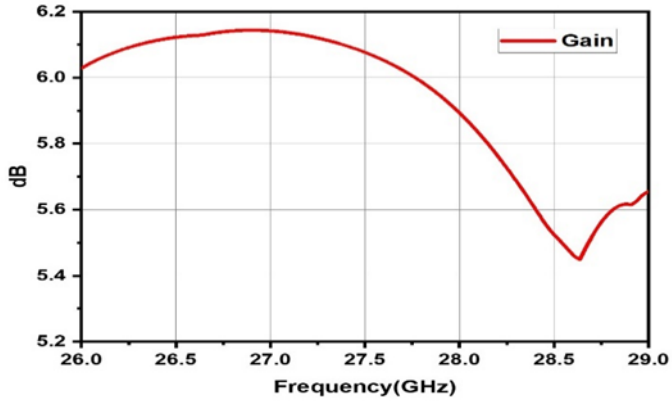

Figure 5. Gain vs Frequency curve of proposed 2 × 9 array antenna**.**

In Fig 5, the gain vs. frequency curve is shown, and the gain is quite stable from 26 to 27.5 GHz. Then it starts to fall and reach a minimum state at 28.636 GHz, but after that, it again increases slowly. At the resonant frequency gain is 5.54 dB.

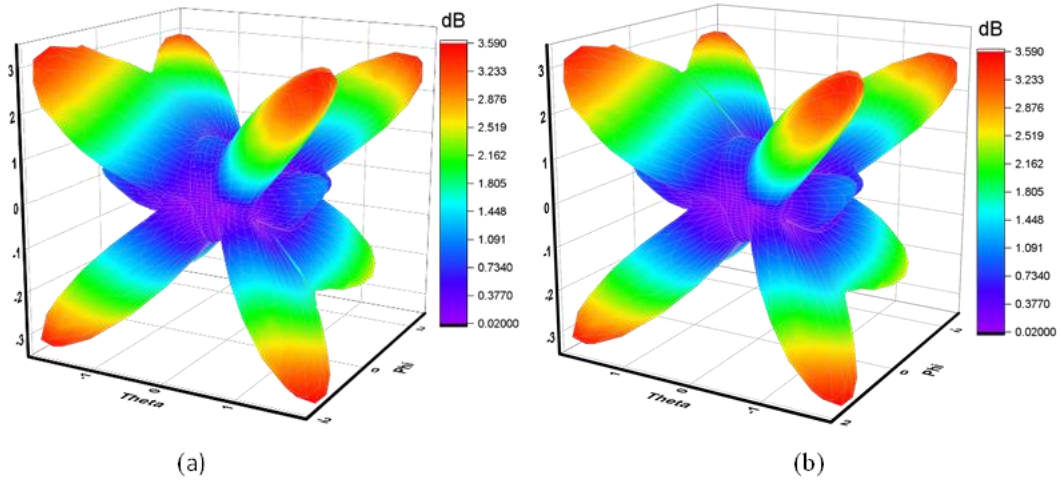

Figure 6. (a) Radiation pattern of port 1 and (b) radiation pattern of port 2 of the proposed antenna.

3D radiation patterns for port 1 and port 2 of the proposed antenna array are presented in Fig 6. The symmetric nature of the design results in nearly mirrored radiation pattern between the upper and lower portions of the antenna array. Besides, both ports show the same radiation pattern. Here are six main lobes that concentrate mainly along the diagonal axes and have higher radiation intensity in these regions. Some side lobes are depicted in the antenna, but the gain is higher in the main lobes. The

mirrored design ensures consistent radiation performance for both ports, which is advantageous for applications like MIMO systems and beamforming networks.

Fig 7 shows the polar plots of the proposed antenna. Plot (a) and (b) show the antenna's radiation pattern at different angles. At (a) where phi = 0, exhibits a multilobe pattern with main lobes at approximately ±30° and nulls at 0° and 180°. The plot of (b), theta = 90 shows a similar multilobe pattern but here the main lobe is at ±60°. These patterns suggest that the antenna radiates power in multiple directions, leading to lower gain in any single direction as the energy is distributed across several lobes. This behavior is quite typical for antennas with wide coverage or multiple main lobes.

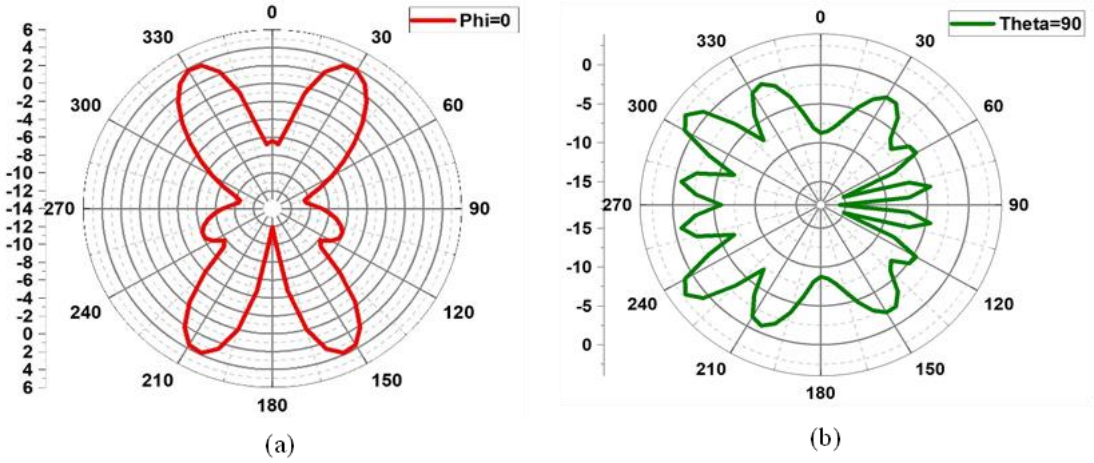

Figure 7. (a) Directivity Phi=0 and (b) directivity Theta=90 of the proposed antenna.

Radiating and total efficiency of the proposed 2 × 9 array antenna.is shown in Fig 8. The radiating efficiency is always higher in the antenna than the total efficiency, but it decreases slowly from 26 to 29 GHz while the total efficiency increases from 26 to 28.5 GHz and then decreases. Radiating efficiency is 84.5% at the resonant frequency, and total efficiency is 82.7%. So, efficiency is quite good as not much of it is lost due to internal issues. Moreover, total efficiency is consistently above 80%, which is a good sign.

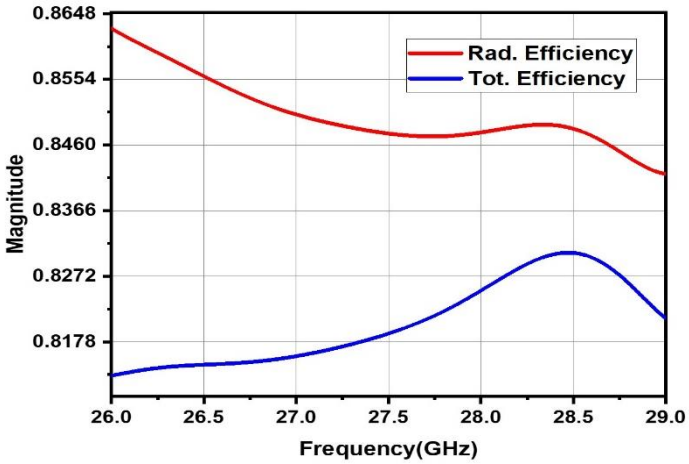

Figure 8. Radiating and total efficiency of the proposed 2 × 9 array antenna.

Fig 9 shows the current distribution of the proposed antenna. In (a), the distribution for port 1 is shown, and in (b) for port 2 is shown. For port 1, strong currents (red, 107 dBmA/m) are concentrated near the feed and the upper and lower edges, which indicates significant excitation and radiation. Moderate to weak currents (green to blue, 66.9-80 dBmA/m) spread across the structure as energy propagates outward. In port 2, the current distribution is similar but shifted. The patterns confirm efficient energy transfer and radiation at both ports, which are critical for antenna performance.

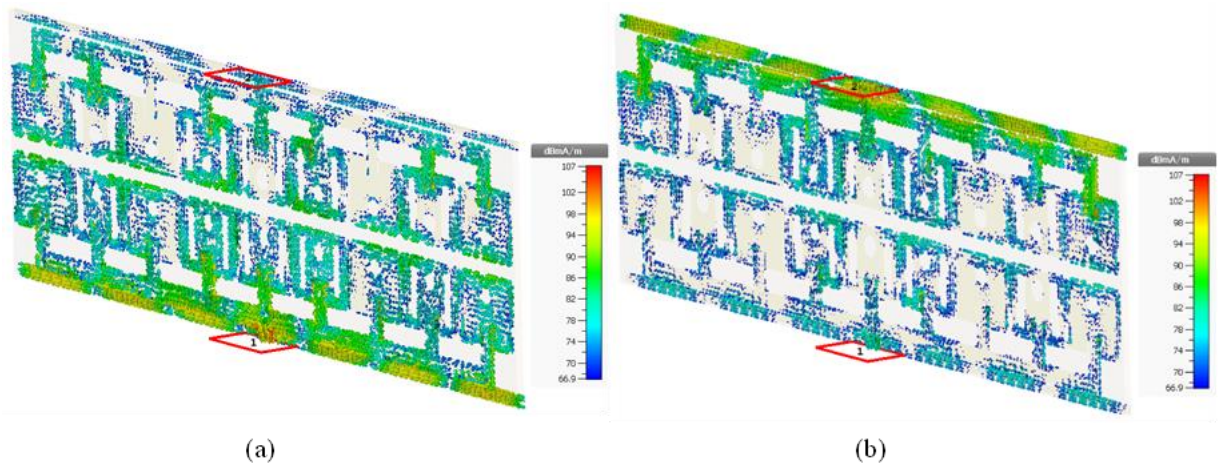

(a) (b)

Figure 9. Surface current of the proposed 2 × 9 array antenna.

4. CONCLUSION

This study focused on the design and evaluation of a wideband microstrip patch array antenna for 5G communication applications. The proposed antenna, designed on a Rogers RT/Duroid5880 substrate with a dielectric constant of 2.2, achieved a return loss of -26.24 dB, gain of 5.54 dB, and total efficiency of 82.7% at the resonant frequency. However, the results are quite stable across the entire bandwidth. It has a bandwidth of 3 GHz. These results show that the antenna meets the performance requirements for next-generation wireless communication systems. This compact and efficient design can be integrated into 5G-enabled devices. Although the antenna shows good results, further optimization can be done to increase its performance in unfavorable environments. Besides, it is just the simulated analysis of the antenna; in the future, by fabricating it, the performance can be measured in real life. Techniques like machine learning can be used for further improvement in performance. The findings of this study contribute to the development of compact and efficient antenna models for modern wireless communication, opening the way for advancements in 5G technology.

5. REFERENCES

Adamiuk, G., Zwick, T., & Wiesbeck, W. (2012). UWB antennas for communication systems. *Proceedings of the IEEE,* 100(7), 2308–2321.

Ahmad, I., Sun, H., Zhang, Y., & Samad, A. (2020). High gain rectangular slot microstrip patch antenna for 5G mm-wave wireless communication. In *2020 5th International Conference on Computer and Communication Systems (ICCCS)*.

Ali, W., Das, S., Medkour, H., & Lakrit, S. (2020). Planar dual-band 27/39 GHz millimeter-wave MIMO antenna for 5G applications. *Microsystem Technologies*, 27(1), 283–292.

Ban, Y.-L., Li, C., Sim, C.-Y.-D., Wu, G., & Wong, K.-L. (2016). 4G/5G multiple antennas for future multi-mode smartphone applications. *IEEE Access,* 4, 2981–2988.

Dixit, A. S., & Kumar, S. (2019, December 9). The enhanced gain and cost-effective antipodal Vivaldi antenna for 5G communication applications. [Journal Name Unavailable].

Girjashankar, P. R., Upadhyaya, T., & Desai, A. (2022). Multiband hybrid MIMO DRA for sub-6 GHz 5G and WiFi-6 applications. *International Journal of RF and Microwave Computer-Aided Engineering, 32*(12), Article 23479.

Hong, T., Zheng, S., Liu, R., & Zhao, W. (2021). Design of mmWave directional antenna for enhanced 5G broadcasting coverage. *Sensors,* 21(3), 746.

Hong, W., Baek, K., Lee, Y.-J., & Kim, Y. (2014). Design and analysis of a low-profile 28 GHz beam steering antenna solution for future 5G cellular applications. *International Microwave Symposium*.

Hong, W., Baek, K.-H., Lee, Y., Kim, Y., & Ko, S.-T. (2014). Study and prototyping of practically large-scale mmWave antenna systems for 5G cellular devices. *IEEE Communications Magazine,* 52(9), 63–69.

Lai, H. W., & Wong, H. (2015). Substrate integrated magneto-electric dipole antenna for 5G Wi-Fi. *IEEE Transactions on Antennas and Propagation,* 63(2), 870–874.

Lai, H. W., & Wong, H. (2015). Substrate integrated magneto-electric dipole antenna for 5G Wi-Fi. *IEEE Transactions on Antennas and Propagation,* 63(2), 870–874.

Li, T., & Zhi Ning Chen. (2020). Shared-surface dual-band antenna for 5G applications. *IEEE Transactions on Antennas and Propagation,* 68(2), 1128–1133.

Lin, Q. W., Wong, H., Zhang, X. Y., & Lai, H. W. (2014). Printed meandering probe-fed circularly polarized patch antenna with wide bandwidth. *IEEE Antennas and Wireless Propagation Letters,* 13, 654–657.

Mak, K. M., Lai, H. W., Luk, K. M., & Chan, C. H. (2014). Circularly polarized patch antenna for future 5G mobile phones. *IEEE Access, 2*, 1521–1529.
Mpele, P. M., Mbango, F. M., & Bernard, D. (2019). A small dual-band (28/38 GHz) elliptical antenna for 5G applications with DGS. *International Journal of Scientific & Technology Research*, *8*(10), 353–357.
Oras Ahmed Shareef, Mohammed, A., Karrar Shakir Muttair, Mahmood Farhan Mosleh, & Mohammad Bashir Almashhdany. (2022). Design of multi-band millimeter wave antenna for 5G smartphones. *Indonesian Journal of Electrical Engineering and Computer Science, 25*(1), 382–387.
Qas Elias, B. B., Soh, P. J., Abdullah Al-Hadi, A., & Vandenbosch, G. A. E. (2020). Design of a compact, wideband, and flexible rhombic antenna using CMA for WBAN/WLAN and 5G applications. *International Journal of Numerical Modelling: Electronic Networks, Devices and Fields, 34*(5).
Raheel, K., Altaf, A., Waheed, A., Kiani, S. H., Sehrai, D. A., Tubbal, F., & Raad, R. (2021). E-Shaped H-Slotted Dual Band mmWave Antenna for 5G Technology. *Electronics,* 10(9), 1019.
Rahman, A., Yi, N. M., Ahmed, A. U., Alam, T., & Singh, M. (2016). A compact 5G antenna printed on manganese zinc ferrite substrate material. *IEICE Electronics Express,* 13(11), 20160377–20160377.
Rana, M. S., & Rahman, M. M. (2022). Design and analysis of microstrip patch antenna for 5G wireless communication systems. *Bulletin of Electrical Engineering and Informatics*. 11(6), 3329~3337
Ray, S. K., & Shrivastava, A. (2018). A triple rectangular slotted microstrip patch antenna for WLAN & WIMAX applications. *International Journal of Antennas,* 4(1/2), 01–08.
S. B. K. (2021). A design and analysis of crown slot patch antennas for 5G applications. *Turkish Journal of Computer and Mathematics Education,* 12(12), 2663–2668.
Sehrai, D. A., Abdullah, M., Altaf, A., Kiani, S. H., Muhammad, F., Tufail, M., Irfan, M., Glowacz, A., & Rahman, S. (2020). A novel high gain wideband MIMO antenna for 5G millimeter wave applications. *Electronics,* 9(6), 1031.
Shamim, S. M., Dina, U. S., Arafin, N., & Sultana, S. (2021). Design of efficient 37 GHz millimeter-wave microstrip patch antenna for 5G mobile application. *Plasmonics*, 16(4), 1417–1425.
Tahseen, H. U., Zheng, Z., & Yang, L. (2021). A single substrate 38 GHz dual antenna array with compact feed network. *IEEJ Transactions on Electrical and Electronic Engineering,* 16(9), 1203–1208.
Tahseen, H. U., Zheng, Z., & Yang, L. (2021). A single substrate 38 GHz dual antenna array with compact feed network. *IEEJ Transactions on Electrical and Electronic Engineering,* 16(9), 1203–1208.
Tarpara, N. M., Rathwa, R. R., & Kotak, N. A. (2018, April). Design of slotted microstrip patch antenna for 5G application. *International Research Journal of Engineering and Technology (IRJET)*, 5(4).
Toma, R. N., Shohagh, I. A., & Hasan, N. (2019). Analysis of the effect of changing height of the substrate of square-shaped microstrip patch antenna on the performance for 5G application. *International Journal of Wireless and Microwave Technologies,* 9(3), 33–45.
Zeain, M. Y., Abu, M. S., Zakaria, Z., Jamal, A., Syahputri, R., Toding, A., & Sriyanto, S. (2020). Design of a wideband strip helical antenna for 5G applications. *Engineering,* 9(5), 1958–1963.
Zhang, J., Bjornson, E., Matthaiou, M., Ng, D. W. K., Yang, H., & Love, D. J. (2020). Prospective multiple antenna technologies for beyond 5G. *IEEE Journal on Selected Areas in Communications*, 38(8), 1637–1660.